Journal of Basrah Researches (Sciences) **51**(2), 34 (2025)
DOI: https://doi.org/10.56714/bjrs.51.2.3

Synthesis, Anti-Breast Cancer Activity Evaluation, and Molecular Docking Study of Cobalt(II) and Ruthenium(III) Complexes Derived from Benzoylthiourea Compounds

Fatima Ghanim Al-Ali, Rafid Humaidan Al-Asadi *

Department of Chemistry, College of Education for Pure Sciences, Basrah University, Basrah, Iraq .

ARTICLE INFO

Received 6 July 2025
Revised 11 August 2025
Accepted 20 August 2025
Published 31 December 2025

Keywords:

Benzoyl Thiourea, Ruthenium, Cobalt, Breast Cancer, Molecular Docking.

Citation: F. G. Al-Ali, R. H. Al-Asadi, J. Basrah Res. (Sci.) **50**(2), 34 (2025). DOI:https://doi.org/10.56714/bjrs.51.2.3

ABSTRACT

A series of cobalt (II) and ruthenium (III) complexes (1–9) incorporating benzoyl thiourea-based ligands was synthesized through the reaction of 4-ethylbenzoylthiourea derivatives with aqueous cobalt and ruthenium salts. In the presence of potassium carbonate (K_2CO_3) in methanol, thiourea molecules acted as bidentate chelating ligands, coordinating through sulfur (S) and oxygen (O) atoms with the metal ions. Cobalt and ruthenium complexes were successfully synthesized and characterized using various analytical techniques, including infrared spectroscopy (FT-IR), thermogravimetric analysis (TGA), magnetic susceptibility measurements, molar conductivity, and UV–Visible spectroscopy. The biological activity of the synthesized complexes was assessed against the MCF-7 breast cancer cell line to evaluate their cytotoxic effects. Among the tested complexes, complex 3 exhibited high percentage of cancer cell inhibition. Furthermore, molecular docking studies revealed that the complex 3 showed the strongest binding affinity toward the selected 5KCV and 3ERT proteins, as evidenced by its lowest binding energy scores and minimal root-mean-square deviation (RMSD) values, indicating stable and favorable interactions with the active sites of these proteins.

1. Introduction

Over the past decade, significant attention has been paid toward the coordination chemistry of transition metal complexes with benzoyl thiourea derivatives. The increasing scientific interest in benzoyl thiourea compounds is predominantly attributed to their distinctive structural characteristics, which confer unique chemical and biological properties, which possess functional groups such as carbonyl, thionyl, and amine moieties [1,2]. Due to their structural flexibility and ability to form diverse coordination geometries, benzoyl thiourea derivatives exhibit selective binding affinities toward a broad range of metal ions. Such these compounds have garnered increasing importance in both coordination chemistry and biomedical research [3]. The coexistence of hard donor atoms (oxygen and nitrogen) and soft donor atoms (sulfur) within their molecular framework enhances their

*Corresponding author email: dr.rafid74@yahoo.com

ISSN: 1817-2695 (Print); 2411-524X (Online)
Online at: https://jou.jobrs.edu.iq

ability to construct potential stable complexes with the selected transition metals [4,5]. Among the various binding modes, a coordination model via sulfur and oxygen donor atoms has been reported as the most favourable, often leading to the formation of more thermodynamically stable complexes compared to those formed by monodentate ligands [6]. In our previous work, we successfully synthesized novel benzoyl thiourea derivatives. Owing to their significant chemical relevance, we extended our work to investigate their coordinating capability with transition metal ions. The coordination complexes with cobalt and ruthenium ions were synthesized successfully with identified molar ratios of 1:2 (M: L) according to coordination chemistry principles, furthermore, the biological activity of the synthesized complexes was evaluated against MCF-7 breast cancer cells using a MTT assay. This study aimed to show the most potent inhibitory compounds. In addition, molecular docking simulations were performed using the MOE software to investigate the interaction mechanisms between the most active complexes and specific receptors in cancer cells. The findings of this study enhance the comprehensive understanding of the biological mechanisms of action of the synthesized complexes at the molecular level, thereby opening new avenues for the design of novel compounds with promising biological activity in future research.

2. Materials and methods

2.1 . Materials and Instruments

The following reagents were used in this experiment: $CoCl_2.6H_2O$, $RuCl_3.xH_2O$ (obtained from Sigma-Aldrich), K_2CO_3 (obtained from Merck). All chemicals were used with a declared purity of 99%. The synthesized complexes were thoroughly characterized using a range of spectroscopic techniques. Infrared measurement was recorded with a range of 400-4000 cm^{-1} (FT-IR−8400S-Shimadzu), TG analysis (SDT Q600 V20.9 Build 20), molar conductivity (DDS-370A), magnetic susceptibility (SDT Q600 V20.9 Build 20), ICP-AES (ICP-OES-Thermo fisher scientific), and UV-visible spectrophotometer of the complexes were studied using (UV_9200 AC 220v 50 Hz). Moreover, the cytotoxic efficacy against breast cancer cells (MCF-7) was evaluated using the MTT assay.

2.2. General procedure for synthesis of ligands (L1-L5)

Five novel ligands derived from 4-ethylbenzoylthiourea were synthesized following a two-step procedure. In the first step, 4-ethylbenzoyl chloride was reacted with potassium thiocyanate (KSCN) under reflux for one hour. The precipitate obtained from the first step, 4-ethylbenzoyl isothiocyanate, was then reacted with various primary aromatic amines under reflux conditions for four hours. The reaction progress was monitored using TLC. Upon completion, the reaction mixture was cooled, and the precipitate was collected by filtration. The crude product was recrystallized from ethanol, followed by drying, melting point determination, and yield calculation.

2.3. General procedure for synthesis of metal complexes.

In a 100 mL conical flask, 10 mmol of each ligand L1–L5 was separately dissolved in 15 mL of methanol. A few drops of the base K_2CO_3 was then added to each ligand to adjust the pH= 8 [7]. Subsequently, (5 mmol) of $CoCl_2.6H_2O$ or $RuCl_3.xH_2O$ dissolved in 5 mL of methanol was gradually added to each ligand solution. The reactions were carried out at room temperature with a continuous stirring for 24 hours. A color change was observed during the reactions, accompanied by precipitate formation. The mixtures were filtered to collect the resulting precipitates, which were then washed several times with water, ethanol, and diethyl ether to remove unreacted materials. The precipitates were then dried and their melting points were measured. Scheme 1. shows the synthesis route of the target complexes and their physical properties are shown in Table 1.

2.4. Cytotoxicity study

The cancer cells incubated with the target complexes were assessed using MTT assay to evaluate their viability [8]. The MTT assay was performed after trypsinizing the cells and adjusted their density to 1.4×10^4 cells/well. The cells were seeded into 96-well plates containing 200 µL of fresh medium per well and incubated for 24 hours to allow the formation of a monolayer. After an incubation process, the cells were treated with different concentrations of the compounds for 24 hours. Subsequently, the supernatant was removed, and 200 µL of MTT solution (0.5 mg/mL in phosphate-buffered saline (PBS)) was added to each well. The plates were then incubated for an additional 4 hours at 37°C. After the incubation, 100 µL of dimethyl sulfoxide (DMSO) was added to dissolve the formazan crystals. Absorbance data were measured at 570 nm using an ELISA reader (BioTek, Model Wave XS2), and the effective concentration of the complexes that causes 50% cell death (IC_{50}) was calculated from the dose-response curves.

3. Results and discussion

Cobalt(II) and ruthenium(III) complexes were synthesized using the prepared ligands with a molar ratio of 1:2 (metal: ligand). Notably, the resulting complexes displayed distinct colors compared to the free ligands, with colour variations observed in the range of dark green to brown and black. These complexes demonstrated thermal stability under ambient conditions as they were obtained in yields ranging from 53% to 75%. Comprehensive characterization was performed employing infrared (IR) spectra, mass spectra, molar conductivity measurements, thermogravimetric analysis (TGA), magnetic susceptibility measurements, and metal: ligand ratio determination.

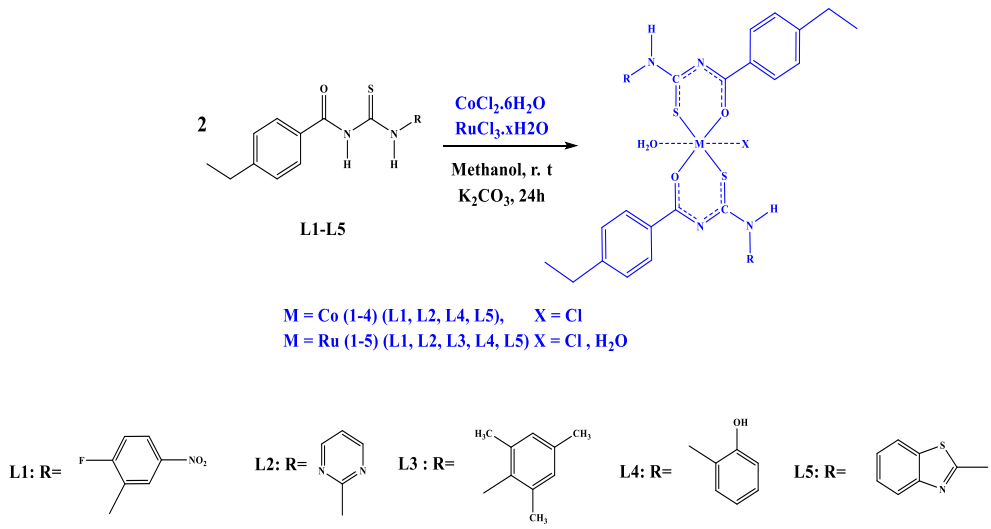

Scheme 1. Synthesis of Co^{+2} and Ru^{+2} complexes.

NMR spectra of synthesized ligands

NMR characterizations of synthesized ligands were recorded using (DMSO-d6 as the solvent using Bruker 400MHz instrument) . ^{1}H-NMR the spectrum exhibited multiple signals in the range of 7.07–8.80 ppm, corresponding to aromatic protons [9]. signals corresponding to the amide group were observed as singlets between 7.07–8.80 ppm, while (-NH) protons appeared as a singlet in the range 14.37–13.57 ppm. The triplet signals was observed in the range of 1.24–1.22 ppm, which is characteristic of ($-CH_3$) protons, and quartet signals in the range 2.70–2.68 ppm due to ($-CH_2$) group[10]. Figure 1 shows the ^{1}H-NMR spectrum of the synthesized ligand L1. The ^{13}C-NMR spectra of ligands spectra showed characteristic signals for the functional groups present. Carbonyl (C=O) and thiocarbonyl (C=S) carbons appeared downfield in the ranges of 169.25–168.38ppm and

181.06–177.80ppm, respectively. Aromatic carbons were observed between 159.37–115.36 ppm. Alkyl carbons (CH_3, CH_2) appeared in the region of 28.67–15.61 ppm [11]. The ^{13}C-NMR spectrum of the synthesized ligand L1 is shown in Figure 2.

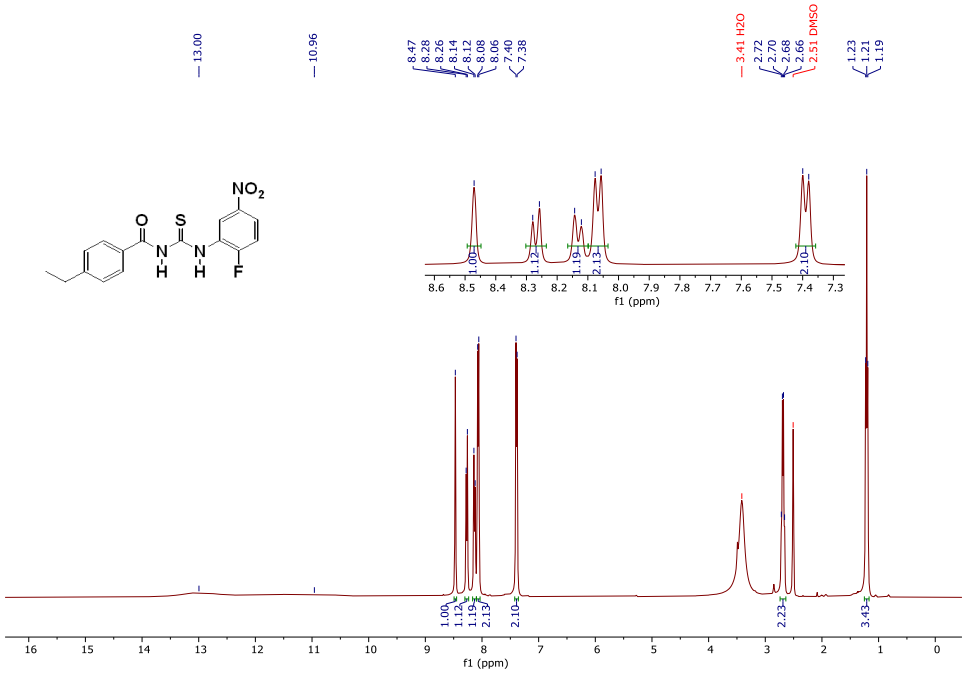

Fig. 1. ^{1}H-NMR spectrum of synthesized L1

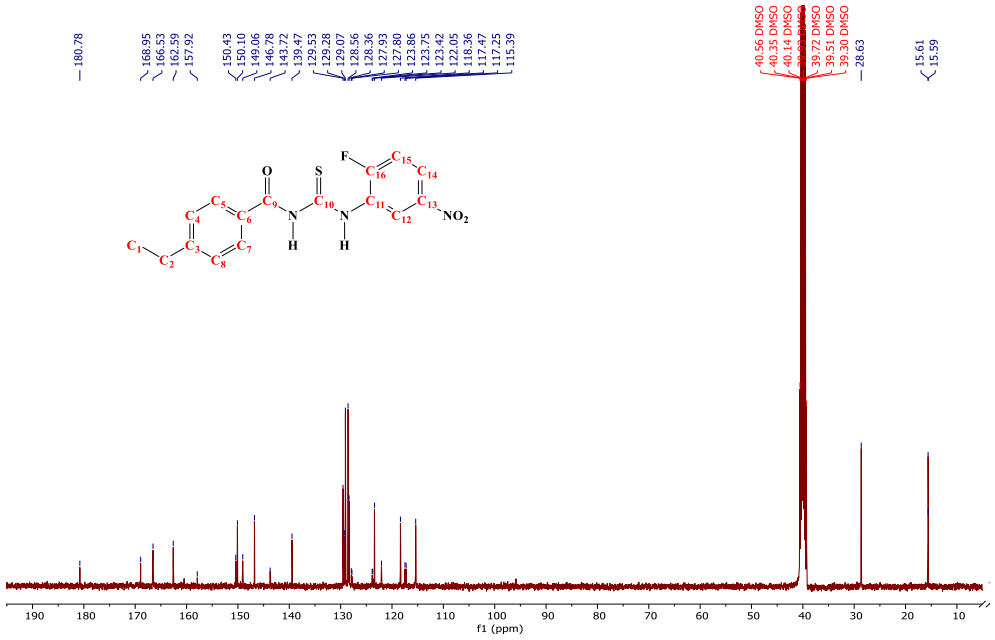

Fig. 2. ^{13}C-NMR spectrum of synthesized L1

IR spectra

The IR spectra of the synthesized ligands showed weak N–H stretching bands at 3130–3336 cm^{-1}. Aromatic C–H stretching appeared at 3001–3097 cm^{-1}. Strong C=O stretching bands were

observed at 1659–1674 cm^{-1}. Additionally, bands of moderate intensity observed in the region of 1606–1465 cm^{-1} were assigned to the C=C stretching vibrations within the aromatic ring structure, while C=S stretching appeared with moderate intensity at 1129–1178cm^{-1}. As an example, Figure 3 presents the IR spectrum of ligand L1.

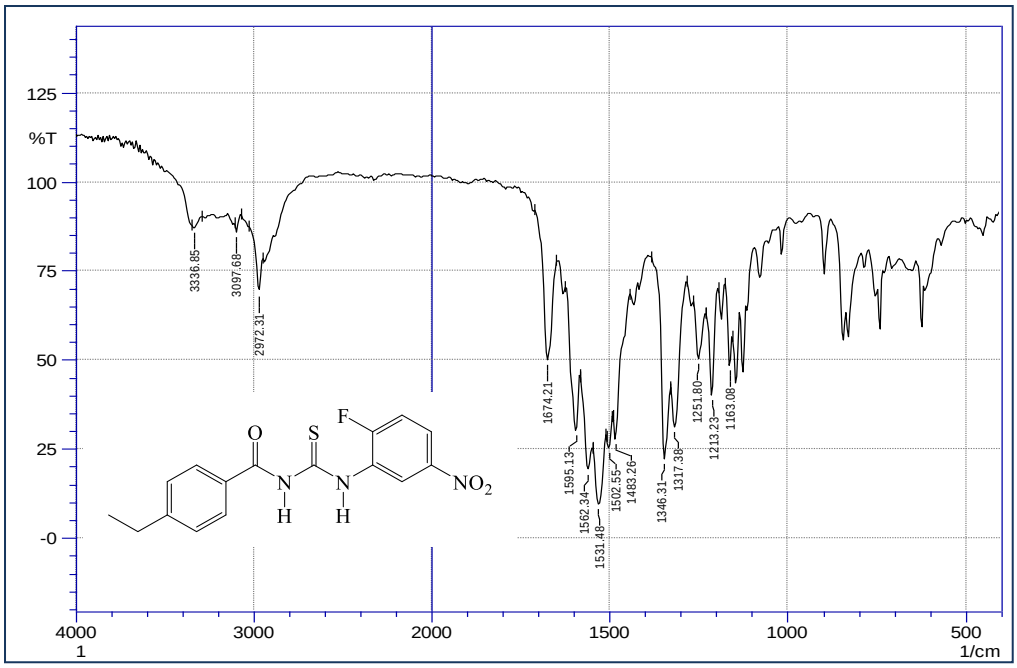

Fig. 3. IR spectrum of ligand L1

IR spectra of all the prepared complexes show characteristic bands in the range of 3216–3397 cm^{-1}, corresponding to the stretching vibration of ν(NH) [12]. Strong vibrations attributed to the ν(C=O) group appeared in the range of 1661 to 1682 cm^{-1}[13,14], the spectra of the complexes showed a shift in the frequency of the (C=O) group, in some complexes, the disappearance of this band was observed The C=O stretching band is observed at 1673 cm^{-1}; however, this band disappears in the case of complex C2. In the ligand L4, the carbonyl stretching band appears at 1662 cm^{-1}, but it is absent in the corresponding complex spectrum, indicating coordination of the carbonyl group with the metal ion. While the thione group ν(C=S) appeared in the range of 1212–1251 cm^{-1}[15]. The appearance of some bands within the same ranges is due to the coordination through sulfur and oxygen atoms with the metal ions. These findings are consistent with the literature [16]. The IR parameters are shown in the Table1.

UV–Visible spectrum

UV-Visible spectra (360–800 nm) of the synthesized complexes were recorded in DMSO at concentrations (5×10^{-3} M) to enable the detection of d-d transitions and to confirm complex formation. The complex 5 exhibited two weak d-d bands at 680 and 630 nm ($A_1g \rightarrow T_2g$ and $A_1g \rightarrow T_1g$), indicating a low-spin octahedral d^6Ru(II) configuration. A strong $\pi \rightarrow \pi^*$ transition appeared below 360 nm, with no charge-transfer bands detected [17]. The complex 6 showed a strong $\pi \rightarrow \pi^*$ band at 370 nm and weak d-d bands at 650 and 630 nm, consistent with a similar low-spin Ru(II) configuration. For Co^{2+} complexes, complex 1 showed a $\pi \rightarrow \pi^*$ transition at 400 nm and a charge-transfer (LMCT) band at 520 nm, while complex 2 exhibited an LMCT band at 560 nm. Both complexes showed d-d transitions at 650,680 nm and 650,620 nm, respectively ($Eg \rightarrow T_1g$ and $Eg \rightarrow T_2g$), with additional shoulders at 670 and 620 nm possibly due to Jahn-Teller distortion [18]. These spectral features confirm that the cobalt complexes adopt distorted low-spin octahedral d^7 configurations as shown in Figure 4 and Table1.

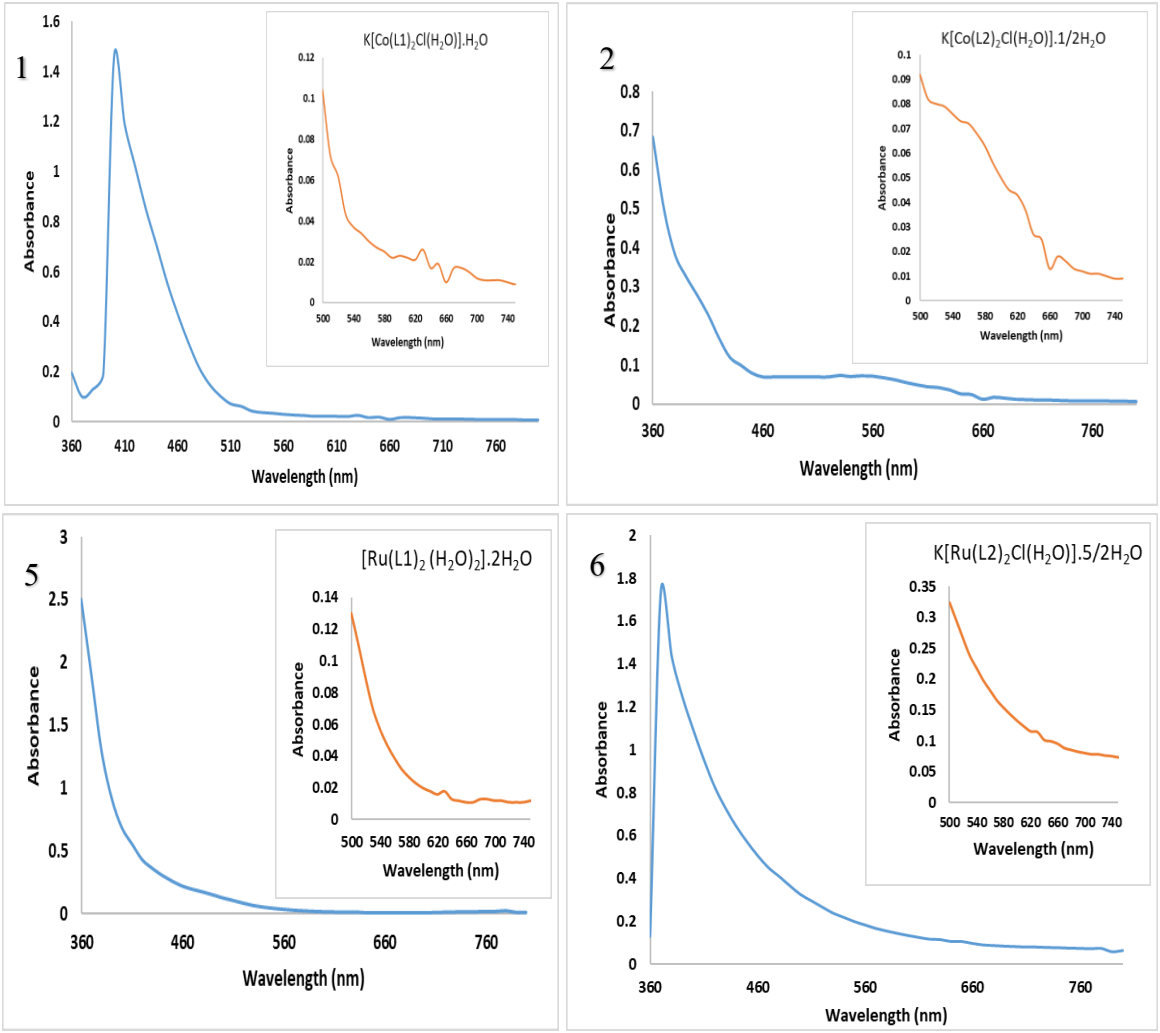

Fig. 4. UV-Vis spectra of complexes 1, 2, 5, 6

Table 1. Physical properties, infrared, and UV data of the target complexes.

No.	Complex	m.p(°C), color	IR			UV
			NH	C=O	C=S	
1	$K[Co(L1)_2Cl(H_2O)].H_2O$	255-253 Yellow	3370	1672	1173	$\pi\rightarrow\pi^*$ ε=1224 CT(M→L) ε=62 d-d($Eg\rightarrow T_1g$) ε=26 d-d($Eg\rightarrow T_2g$) ε=19
2	$K[Co(L2)_2Cl(H_2O)].1/2H_2O$	243-242 Dark green	3216	…..	1087	CT(M→L) ε=72 d-d($Eg\rightarrow T_1g$) ε=25 d-d($Eg\rightarrow T_2g$) ε=18
3	$K[Co(L4)_2Cl(H_2O)].5/2H_2O$	dec. 183 Black	3326	…..	1150	

4	$K[Co(L5)_2Cl(H_2O)].1/2H_2O$	242-240 Dark green	3397	1682	1174	
5	$[Ru(L1)_2(H_2O)_2].2H_2O$	209-210 Brown	3318	1673	1176	d-d($A_1g \rightarrow T_2g$) ε=13 d-d($A_1g \rightarrow T_1g$) ε=18
6	$K[Ru(L2)_2Cl(H_2O)].5/2H_2O$	215-217 Dark brown	3219	1661	1179	π→π* ε=1737 d-d($A_1g \rightarrow T_2g$) ε=114 d-d($A_1g \rightarrow T_1g$) ε=105
7	$K[Ru(L3)_2Cl(H_2O)].4H_2O$	dec.194 Brown	3221	1663	1178	
8	$K[Ru(L4)_2Cl(H_2O)].H_2O$	300< Black	3230	1665	1178	
9	$K[Ru(L5)_2Cl(H_2O)].H_2O$	dec. 212 Dark green	3371	1673	1172	

Magnetic properties

In the magnetic susceptibility measurements, Table 2 shows that cobalt(II) complexes are paramagnetic due to the presence of a single unpaired electron with effective magnetic moments ranging from 1.45 to 1.96 B.M. The reason for the decrease in the effective magnetic moment (μ_{eff}) may be due to the antiferromagnetic effect [19]. This confirms a low-spin d^7 configuration, indicating strong-field ligands and suggesting a distorted octahedral geometry with sp^3d^2 hybridization (outer orbital complexes) [20], and the electronic configuration of Co(II) is [Ar] $3d^74s^0$. In contrast, Ru(III) complexes exhibited diamagnetic behaviour (μ_{eff} = 0.0 B.M), indicating a reduction of Ru(III) to Ru (II) during complex formation [21]. Thus, Ru(II) likely adopts a low-spin configuration with the electronic configuration [Kr] $4d^5$ $5s^0$ and an octahedral geometry with d^2sp^3 hybridization (inner orbital complexes). An exception is the complex 9, which showed paramagnetic properties with a magnetic moment of 1.54 B.M., indicating Ru remains in the +3 oxidation state, with a low-spin d^5 configuration and d^2sp^3 hybridization (octahedral-inner orbital complexes).

ICP-AES (mole ratio)

Determination of the metal content in coordination complexes is essential for confirming their structural framework and proposing the molecular formula. This is typically achieved using inductively coupled plasma (ICP) spectroscopy, where high-temperature plasma (6000–10000 K) generated by radio frequency excitation ionizes the sample atoms. As the excited atoms return to their ground state, they emit element-specific optical spectra, enabling accurate metal quantification. The experimental metal percentages closely matched theoretical values, confirming the consistency of metal :ligand ratio [1:2] [M: L] through all synthesized complexes [22, 23] as shown in Table 2.

Molar Conductivity

The molar conductivity of the complexes were measured using DMSO as a solvent at a concentration of 1×10^{-3} M. The study revealed that the prepared cobalt (II) and ruthenium (III) complexes exhibit variation in molar conductivity, with values ranging between 24.2 and 64.5 ($\mu S \cdot cm^2 \cdot mol^{-1}$). This variation indicates differences in the degree of ionization or dissociation of the dissolved compounds in DMSO. The results suggest that all the prepared complexes behave as 1:1

electrolytes, except for complex 5 which was non-electrolytic as indicated by its low conductivity value of 24.2 ($\mu S \cdot cm^2 \cdot mol^{-1}$) [24] as shown in Table 2.

Table 2. Molar conductivity, ICP-AES and magnetic susceptibility of the target complexes.

No.	Complex	Molar Conductivity Λm ($\mu S.cm^2/mol$)	ICP-AES (mole ratio)		Magnetic Susceptibility	
			Found	Calc.	magnetic moment (μ_{eff})	Number of unpaired electrons (n)
1	$K[Co(L1)_2Cl(H_2O)].H_2O$	36.3	7.32	6.83	1.67	1
2	$K[Co(L2)_2Cl(H_2O)].1/2H_2O$	37.2	10.53	7.86	1.73	1
3	$K[Co(L4)_2Cl(H_2O)].5/2H_2O$	48.5	8.18	7.41	1.91	1
4	$K[Co(L5)_2Cl(H_2O)].1/2H_2O$	49.6	6.19	7	1.52	1
5	$[Ru(L1)_2(H_2O)_2].2H_2O$	24.2	11.36	11.67	0	0
6	$K[Ru(L2)_2Cl(H_2O)].5/2H_2O$	30.8	12.35	12.48	0	0
7	$K[Ru(L3)_2Cl(H_2O)].4H_2O$	64.5	12.59	11.02	0	0
8	$K[Ru(L4)_2Cl(H_2O)].H_2O$	48.2	13.98	12.47	0	0
9	$K[Ru(L5)_2Cl(H_2O)].H_2O$	40.4	10.87	11.30	1.54	1

Thermogravimetric analysis

TGA data of the synthesized complexes were collected over the temperature range of 25–800 °C. The decomposition steps, temperature ranges, mass loss products, and percentage losses at each stage are detailed in Table 3. TGA curves reveal that both cobalt and ruthenium complexes decomposed in three to five stages. The first and second stages (60–220 °C) correspond to the loss of crystallization and coordinated water molecules. The third and fourth stages involve the loss of anionic species such as F^-, NO_2^-, and Cl^-, along with partial degradation of the ligand. The final stage, occurring at higher temperatures, corresponds to the formation of metal residues and metal oxides. The curves indicate variability in decomposition behaviour among the complexes. All complexes showed thermal stability, with complex 3 being the most thermally stable, exhibiting only 38% total mass loss. In contrast, other complexes showed total mass losses ranging from 62% to 84%. This variation is attributed to factors such as electronic structure, bond strength, and geometric stability of the complexes [25, 26] as shown in Table 3.

Table 3. TGA of the synthesized complexes.

No.	Complex	Temp. (°C)	Decomposition steps	Weight loss %	
				Calculated	found
1	$K[Co(L1)_2Cl(H_2O)].H_2O$	185-220	$2H_2O+K$	8.68	8.77
		230-320	2F+Cl	9.01	9.27
		330-380	CH_3+NO_2	8.50	8.38
		380-475	C_8H_{10}	16.15	17.02
		485-575	$2(C_6H_4CO)$	38.16	38.78

2	$K[Co(L2)_2Cl(H_2O)]$ $.1/2H_2O$	180-280	$3/2H_2O+Cl+K+C_9H_9$	29.10	28.84
		280-510	C_8H_{10}	19.95	19.27
		270-805	$C_2H_2N_2SO$	24.70	24.69
3	$K[Co(L4)_2Cl(H_2O)]$ $.5/2H_2O$	60-155	H_2O	2.26	2.60
		160-470	$5/2H_2O+Cl+K+C_9H_{10}NO$	38.21	38.15
		475-795	C_6H_6O	19.57	21.03
4	$K[Co(L5)_2Cl(H_2O)]$ $.1/2H_2O$	100-160	$1/2H_2O$	0.93	1.010
		180-300	$H_2O+C_8H_{10}$	13.08	12.95
		300-490	$Cl+K+C_9H_{10}NO$	26.90	26.94
		500-690	$C_7H_5N_2S$	24.70	24.32
5	$[Ru(L1)_2(H_2O)_2]$ $.2H_2O$	130-340	$4H_2O+C_8H_5FN_3O_3S+NO_2$	41.62	42.29
		350-500	$C_{10}H_{12}N_2OS$	41.18	41.76
6	$K[Ru(L2)_2Cl(H_2O)]$ $.5/2H_2O$	150-310	$7/2H_2O+Cl+K+2(C_8H_{10})$	43.12	43.30
		310-460	$C_9H_{11}NO+CH_3$	35.63	35.54
7	$K[Ru(L3)_2Cl(H_2O)]$ $.4H_2O$	160-310	$Cl+5H_2O+K+C_{19}H_{21}N_2OS$	61.48	61.28
		430-510	$+CH_3N_2S$ CH_3	4.25	6.901
8	$K[Ru(L4)_2Cl(H_2O)]$ $.H_2O$	130-270	$2H_2O+K$	9.25	9.47
		280-390	CH_3N_2S+Cl	14.61	15.05
		400-550	C_6H_6O	14.63	14.24
9	$K[Ru(L5)_2Cl(H_2O)]$ $.H_2O$	130-200	$2H_2O$	3.57	3.64
		200-320	C_7H_6+K+Cl	20.15	19.76
		330-410	CH_4N_2S	10.66	10.85
		425-600	$C_{10}H_{11}N_2OS$	32.46	33.92

Anti-cancer Activity

The study of the biological activity of complexes is a crucial step for evaluating their potential as anticancer agents. In this research, the anti-breast cancer activity of complexes 1, complex 3, complex 4, complex 6, complex 8, complex 9 were evaluated using the MCF-7 breast cancer cell line. Five different concentrations (4.7, 22.22, 66.66, 200, and 600 µg/mL) were used to assess the inhibitory effects for each complex on cell growth. The IC_{50} values (a concentration required to inhibit 50% of cell viability) were calculated for each complex. The results showed that all complexes exhibited concentration-dependent inhibition, suggesting varying levels of anticancer activity. Complex 3 showed the highest inhibitory effects with IC_{50} values of 14.96 µg/mL. This enhanced activity is attributed to the electron-donating nature of the hydroxyl (OH) group, which

increases the molecule's ability to form hydrogen bonds. These interactions may improve the compound's ability to bind to intracellular proteins and facilitate easier penetration through cell membrane [27] as shown in Table 4.

Table 4. IC_{50} values of the studied compounds against MCF-7 cell line

No.	Complexes	Conc.(µg /mL)					IC_{50} (µg /mL)
		7.4	22.22	66.66	200	600	
		Cells inhibition (%)					
1	$K[Co(L2)_2Cl(H_2O)].1/2H_2O$	6.15	13.74	24.1	44.06	67.61	257
3	$K[Co(L4)_2Cl(H_2O)].5/2H_2O$	37.3	56.91	73.16	79.28	89.21	14.96
4	$K[Co(L5)_2Cl(H_2O)].1/2H_2O$	8.09	17.57	29.87	35.39	56.12	486.98
6	$K[Ru(L2)_2Cl(H_2O)].5/2H_2O$	3.68	15.59	19.93	35.53	44.21	150.54
8	$K[Ru(L4)_2Cl(H_2O)].H_2O$	4.74	34.41	47.83	58.29	73.09	102.65
9	$K[Ru(L5)_2Cl(H_2O)].H_2O$	15	29.01	44.01	52.69	57.89	187.26

Molecular Docking Study

Molecular docking was conducted for the compounds that showed the highest inhibitory activity against breast cancer (MCF-7) cell line proteins by using the program (MOE 2019), namely cobalt complex (3)[28,29]. The crystal structures of the key proteins involved in this type of cancer were obtained from the Protein Data Bank (PDB) (https://www.rcsb.org/structure), including: Akt (PDB ID: 5KCV), EGFR (PDB ID: 2J6M), PR(PDB ID: 4OAR), mTOR(PDB ID: 4DRH), CDK6(PDB ID: 3NUP), CDK2(PDB ID: 4FX3), ERα (PDB ID: 3ERT) [30, 31]. Molecular docking was performed following established protocols from the literature [32, 33]. The protein structures were prepared by removing water molecules, and optimizing the geometry. The ligand structures were energy-minimized and spatially optimized before initiating the docking process. The docking results showed that the complex 3 offered the strongest binding interactions with Akt (5KCV) and receptor alpha (3ERT).

In the interaction of the complex 3 with the target proteins, it exhibited the lowest binding energy, indicating that its binding was more stable. The observed stability could be ascribed to the extended molecular framework and the high density of active functional groups within the structure. Two main interactions were observed with 3ERT receptor: the first one is a hydrogen bond donor interaction between the chlorine atom of complex and amino acid Cys-530. The second one is a π- π interaction between the phenyl ring and amino acid Thr-347 *via* van der Waals interactions involving 18 amino acid residues. For the 5KCV protein, four main interactions were observed as three hydrogen bonds appeared with amino acids Asp-274, Cys-296, and Tyr-18, one π- π interaction between the phenyl ring and Gly-18 in addition to van der Waals interactions with 13 amino acid residues as detailed in Table 5 and Figures 5 and 6.

Table 5. Molecular docking data of $K[Co(L4)_2Cl(H_2O)].5/2H_2O$ with 3ERT and 5KCV proteins.

proteins (Recepter)	RMSD(Å)	Affinity energy (S) Kcal/mol	Interaction		
			Type	Amino acid	Distance (Å)

3ERT	1.721	-8.631	H-bond donor *pi*-H	Cys 530 Thr 347	3.39 4.28
5KCV	1.966	-7.202	H-bond donor H-bond acceptor H-bond acceptor *pi*-H	Asp 274 Cys 296 Tyr 18 Gly 294	2.64 3.70 3.16 4.60

Conclusion

A series of coordination complexes of divalent cobalt and trivalent ruthenium derived from 4-ethylbenzoyl ligands was synthesized to form stable complexes. Spectroscopic and analytical data confirmed that all ligands act as bidentate donors through O and S atoms. Thermal analysis results revealed that most of the complexes exhibited good thermal stability and contain crystallization water molecules located outside the coordination sphere. Molar conductivity measurements revealed that the synthesized complexes behave as electrolytes in solution, indicating the dissociation of the complexes into their ionic constituents and the presence of free external ions. The experimental percentage values of the metals show strong agreement with the theoretical values based on the proposed molecular formulas, supporting a consistent metal to ligand ratio of [2:1] in all the synthesized complexes. Electronic spectra and magnetic susceptibility measurements demonstrated that the cobalt (II) complexes are paramagnetic, with a distorted octahedral geometry and sp^3d^2 hybridization. In contrast, Ru(III) was reduced to Ru(II) during complex formation, and the resulting ruthenium(II) complexes exhibited diamagnetic properties and an octahedral geometry with d^2sp^3 hybridization .The results of the biological assays against MCF-7 breast cancer cells indicated that the compounds exhibited low inhibition values, which increased with increasing concentration, indicating that these compounds possess varying degrees of inhibitory activity. The complex 3 containing OH group demonstrated the highest inhibitory effect among the studied compounds, with an IC_{50} value of 14.96 µg/mL. Molecular docking studies revealed that the interaction of the complex 3 with the proteins 3ERT and KCV5 resulted in the lowest binding energy (S) and the lowest RMSD values, indicating a more stable binding interaction. This may be attributed to the large size of the complex and the presence of multiple active functional groups.

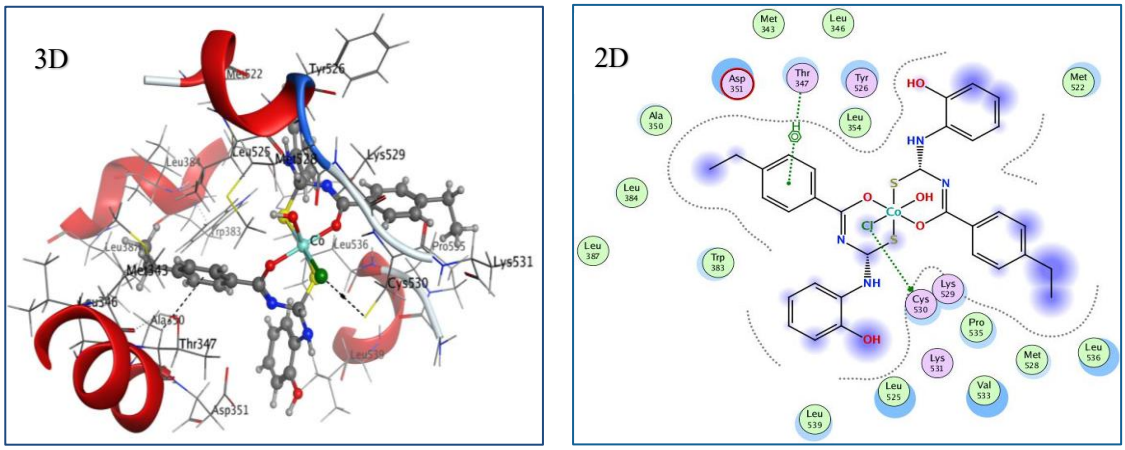

Fig. 5. 2D and 3D forms of the binding of the complex $K[Co(L4)_2Cl(H_2O)].5/2H_2O$ with the 3ERT protein.

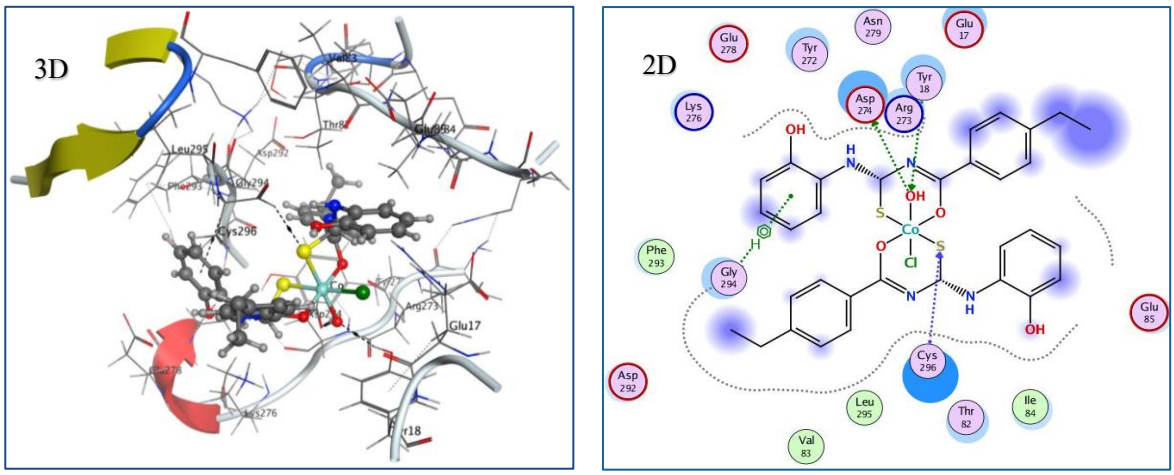

Fig. 6.2D and 3D forms of the binding of the complex $K[Co(L4)_2Cl(H_2O)].5/2H_2O$ with the 5KCV protein.

References

[1] J.-J. Wei, J.-J. Xiao, J.-W. Yu, X.-Y. Yi, S. Liu, and G.-Y. Liu, "Synthesis and structural characterization of silver (I) and gold (I) complexes of N, N′-diisobutyloxycarbonyl-N″, N‴-(1,3-propylene)-bisthiourea," Polyhedron, vol. 137, pp. 176–181, 2017. DOI:10.1016/j.poly.2017.08.014

[2] A. Farook and A. Nadiah, "The Synthesis and Characterisation of 2-methyl-N-((4-methylpyridine-2-yl)carbamothiol)benzamide: Its Preparation with Antibacterial Study," J. Phys. Sci., vol. 27, no. 2, pp. 83–101, 2016. DOI: 10.21315/jps2016.27.2.7

[3] U. A. Khan, A. Badshah, M. N. Tahir, and E. Khan, "Gold (I), silver (I) and copper (I) complexes of 2,4,6-trimethylphenyl-3-benzoylthiourea; synthesis and biological applications," *Polyhedron*, vol. 181, p. 114485, 2020. DOI:10.1016/j.poly.2020.114485

[4] H. B. Mohammed Shawish, "Synthesis, characterization and biological studies of nickel (II) complexes containing thiosemicarbazone and thiourea derivatives," Ph.D. dissertation, Univ. of Malaya, Malaysia, 2014.

[5] L. Beyer, E. Hoyer, J. Liebscher, and H. Hartmann, "Komplexbildung mit N-Acyl-thioharnstoffen," *Zeitschrift für Chemie*, vol. 21, no. 3, pp. 81–91, 1981. DOI:10.1002/zfch.19810210302

[6] S. Aamer, F. Ulrich, and F. Mauricio, "A review on the chemistry, coordination, structure and biological properties of 1-(acyl/aroyl)-3(substituted) thioureas," *J. Sulfur Chem.*, vol. 35, no. 3, pp. 318–355, 2014. DOI:10.1080/17415993.2013.834904

[7] M. Iliş, M. Micutz, and V. Cîrcu, "Luminescent palladium (II) metallomesogens based on cyclometalated Schiff bases and N-benzoyl thiourea derivatives as co-ligands," *J. Organomet. Chem.*, vol. 836, pp. 81–89, 2017. DOI:10.1016/j.jorganchem.2017.03.015

[8] R. Abedalhusaeen and H. Rafid, "Synthesis, Characterization, DFT, Molecular Docking Studies and Evaluation of Biological Activity of Benzamidethiourea Derivatives against HepG2 Hepatocellular Carcinoma Cell Lines," *Adv. J. Chem., Sect. A*, vol. 2025. DOI: 10.48309/AJCA.2025.464453.1575

[9] F. Faye, R. Sylla-Gueye, I. E. Thiam, J. Orton, S. Coles, and M. Gaye, "Synthesis, Characterization and Crystal Structure of 1-(2-benzamidophenyl)-3-benzoylthiourea Hemihydrate," *Sci. J. Chem.*, vol. 8, no. 6, pp. 131–135, 2020. DOI: 10.11648/j.sjc.20200806.11

[10] M. Marzi, K. Pourshamsian, F. Hatamjafari, A. Shiroudi, and A. R. Oliaey, "Synthesis of new N-Benzoyl-N'-triazine thiourea derivatives and their antibacterial activity," *Russ. J. Bioorg. Chem.*, vol. 45, no. 5, pp. 391–397, 2019. DOI: 10.1134/S106816201905008X

[11] C. K. Ozer, G. Binzet, and H. Arslan, "Crystal and Molecular Structure of bis(N-(diethylcarbamothioyl)cyclohexane carboxamido) copper (II) Complex," *Eur. J. Chem.*, vol. 11, pp. 319–323, 2020. DOI: https://doi.org/10.5155/eurjchem.11.4.319-323.2047

[12] M. J. Meften and A. A. Kadhim, "Synthesis of 5-benzyl-5-((5-nitropyridin-3yl)methyl)-1,3,5-dithiazinan-5-ium through one-pot reactions, characterization and study as a corrosion retardant in high salinity oil fields," *Basrah Res. Sci.*, vol. 49, no. 2, pp. 140–163, 2023.DOI:https://doi.org/10.56714/bjrs.49.2.12

[13] M. J. Mohammed, U. J. Al-Hamdani, and R. A. Alharis, "Preparation and characterization of Schiff base and its complex with Cu (II) and study of their liquid crystalline properties," *Basrah Res. Sci.*, vol. 49, no. 2, pp. 22–29, 2023. DOI: https://doi.org/10.56714/bjrs.49.2.3

[14] O. W. Adesina, O. J. Ayoola, B. U. Muham, and A. M. Olabisi, "Octahedral platinum (IV) complexes of pyrimethamine: synthesis, spectros," *Res. J. Chem.*, vol. 9, no. 3, pp. 24–39, 2019.

[15] A. M. Alkherraz, Z. I. Lusta, and A. E. Zubi, "Synthesis and use of thiourea derivative (1-phenyl-3-benzoyl-2-thiourea) for extraction of cadmium ion," *Int. J. Chem. Nucl. Metall. Mater. Eng.*, vol. 8, pp. 118–120, 2014. Available: http://waset.org/publications/9997379/

[16] C. Avşar, B. T. Findik, B. Dede, M. Erdem-Tuncmen, and F. Karipcin, "Transition metal complexes of N-furfuryl-N′-benzoylthiourea: A study of synthesis, antibacterial activities, quantum chemical calculations and molecular modeling simulations," *Polyhedron*, vol. 267, p. 117357, 2025. DOI:https://doi.org/10.1016/j.poly.2024.117357.

[17] A. A. Al-Riyahee, "An exploration of the synthesis, coordination chemistry and properties of novel thiourea ligands and their complexes," Ph.D. dissertation, Cardiff Univ., 2016. Available: https://orca.cardiff.ac.uk/id/eprint/94404

[18] A. M. Shalash and H. I. Abu Ali, "Synthesis, crystallographic, spectroscopic studies and biological activity of new cobalt (II) complexes with bioactive mixed sulindac and nitrogen-donor ligands," *Chem. Cent. J.*, vol. 11, no. 1, p. 40, 2017. DOI 10.1186/s13065-017-0268-2

[19] Y. M. Al-Salim and R. H. Al-Asadi, "Synthesis, Anti-breast Cancer Activity, and Molecular Docking Studies of Thiourea Benzamide Derivatives and Their Complexes with Copper Ion," *Trop. J. Nat. Prod. Res.*, vol. 7, no. 6, 2023. DOI:10.26538/tjnpr/v7i6.15.

[20] A. Kumar, "Study on Magnetic Susceptibility of Co (II) Complexes and Electronic Spectra of Co (II) Complexes," *Int. J. Innov. Eng. Res. Technol.*, vol. 8, no. 12, pp. 88–92, 2021. DOI: 10.17605/OSF.IO/SBVCX

[21] M. E. Uysal, U. Solmaz, and H. Arslan, "Ruthenium (III) acyl thiourea complex: A catalyst for transfer hydrogenation of nitroarenes," *Polyhedron*, vol. 247, p. 116707, 2024. DOI:10.1016/j.poly.2023.116707

[22] I. P. Paktsevanidou, N. Manousi, and G. A. Zachariadis, "Development and validation of an inductively coupled plasma–atomic emission spectrometry (ICP-AES) method for trace element determination in vinegar," *Anal. Lett.*, vol. 54, no. 13, pp. 2227–2238, 2021. DOI:10.1080/00032719.2020.1854777

[23] K. Jusufi, T. Stafilov, M. Vasjari, B. Korça, J. Halili, and A. Berisha, "Determination of heavy metals by ICP-AES in the agricultural soils surrounding Kosovo's power plants," *Fresenius Environ. Bull.*, vol. 25, pp. 1312–1320, 2016.

[24] M. S. Refat, I. M. El-Deen, M. A. Zein, A. M. A. Adam, and M. I. Kobeasy, "Spectroscopic, structural and electrical conductivity studies of Co (II), Ni (II) and Cu (II) complexes derived from 4-acetylpyridine with thiosemicarbazide," *Int. J. Electrochem. Sci.*, vol. 8, no. 7, pp. 9894–9917, 2013.

[25] R. K. K. Reddy, P. Suneetha, C. S. Karigar, N. H. Manjunath, and K. N. Mahendra, "Cobalt (II), Ni (II), Cu (II), Zn (II), Cd (II), Hg (II), UO_2 (VI) and Th (IV) complexes from ONNN Schiff base ligand," *J. Chil. Chem. Soc.*, vol. 53, no. 4, pp. 1653–1657, 2008. DOI:10.4067/S0717-97072008000400003.

[26] C. R. Bhattacharjee, P. Goswami, and P. Mondal, "Synthesis, reactivity, thermal, electrochemical and magnetic studies on iron (III) complexes of tetradentate Schiff base ligands," *Inorg. Chim. Acta*, vol. 387, pp. 86–92, 2012. DOI:10.1016/j.ica.2011.12.056

[27] T. O. Brito, L. O. Abreu, K. M. Gomes, M. C. S. Lourenço, P. M. L. Pereira, S. F. Yamada-Ogatta, Â. de Fátima, C. A. Tisher, F. M. Jr, and M. L. F. Bispo, "Benzoylthioureas: Design, synthesis and antimycobacterial evaluation," *Med. Chem.*, vol. 16, no. 1, pp. 93–103, 2020.DOI: https://doi.org/10.2174/1573406415666181208110753

[28] A. T. Nasser and R. H. Al-Asadi, "Schiff Bases Ligands Derived from o-Phthalaldehyde and Their Metal Complexes with Cu^{2+} and Ni^{2+}: Synthesis, Anti-Breast Cancer and Molecular Docking Study," *Trend Sci.*, vol. 20, no. 9, p. 5675, 2023. DOI: https://doi.org/10.48048/tis.2023.5675

[29] C. Scholz, S. Knorr, K. Hamacher, and B. Schmidt, "DOCKTITE—A Highly Versatile Step-by-Step Workflow for Covalent Docking and Virtual Screening in the Molecular Operating Environment," *J. Chem. Inf. Model.*, vol. 55, no. 2, pp. 398–406, 2015. DOI:10.1021/ci500681r

[30] L. Veterini, A. D. Savitri, M. S. Widyaswari, M. R. Akbar, A. Fairus, M. Q. B. Zulfikar, M. Astri, N. A. Ramasima, and D. P. Anggraeni, "In silico study of the potential of garlic allicin compound as anti-angiogenesis," *Trop. J. Nat. Prod. Res.*, vol. 5, no. 11, pp. 1995–1999, 2021. [Online]. Available: DOI: http://repository.unusa.ac.id/id/eprint/8599

[31] C. Dong, J. Wu, Y. Chen, J. Nie, and C. Chen, "Activation of PI3K/AKT/mTOR pathway causes drug resistance in breast cancer," *Front. Pharmacol.*, vol. 12, p. 628690, 2021. DOI: 10.3389/fphar.2021.628690

[32] M. K. Mohammed, F. A. Almasha, H. H. Al-hujaj, R. H. Al-asadi, H. A. Jaber, A. M. Jassem, and H. Dhaef, "Synthesis, Characterization, Cytotoxic Evaluation on MCF-7 Breast Cancer Cells, and Theoretical Studies of Novel 1,2,3-Triazoles," *Trop. J. Nat. Prod. Res.*, vol. 8, no. 10, 2024. DOI: https://doi.org/10.26538/tjnpr/v8i10.22

[33] N. A. Elkanzi, M. A. Ali, M. Albqmi, and A. Abdou, "New Benzimidazole-Based Fe (III) and Cr (III) Complexes: Characterization, Bioactivity Screening, and Theoretical Implementations Using DFT and Molecular Docking Analysis," *Appl. Organomet. Chem.*, vol. 36, no. 11, p. e6868, 2022. DOI: https://doi.org/10.1002/aoc.6868

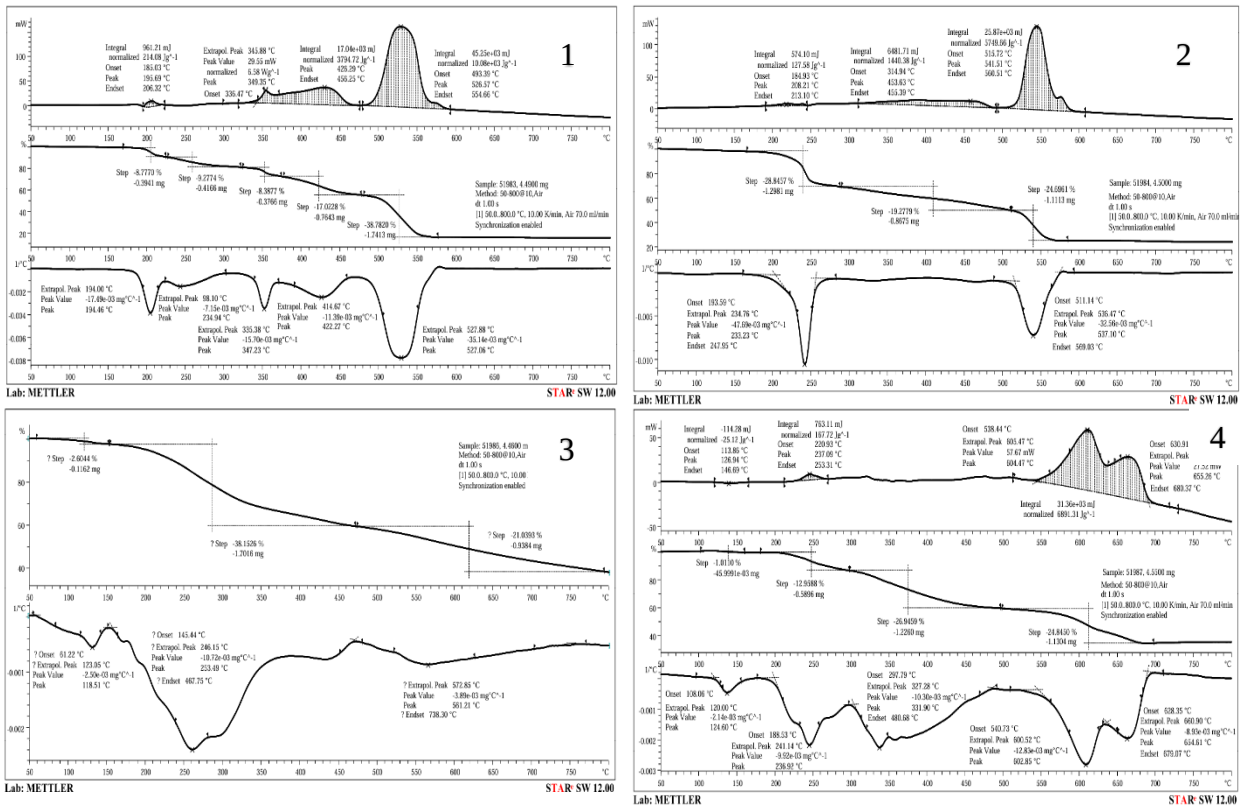

TGA spectra of complexes 1-4

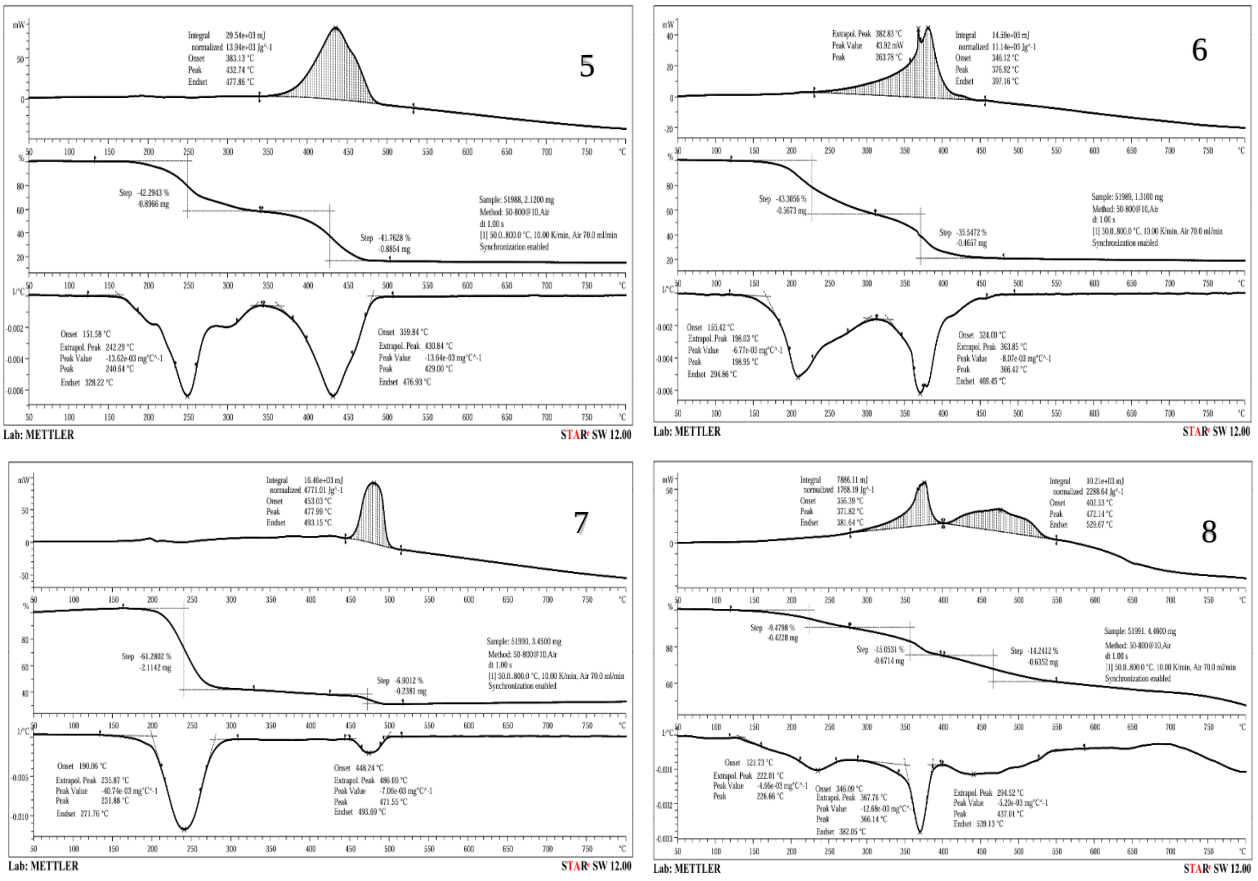

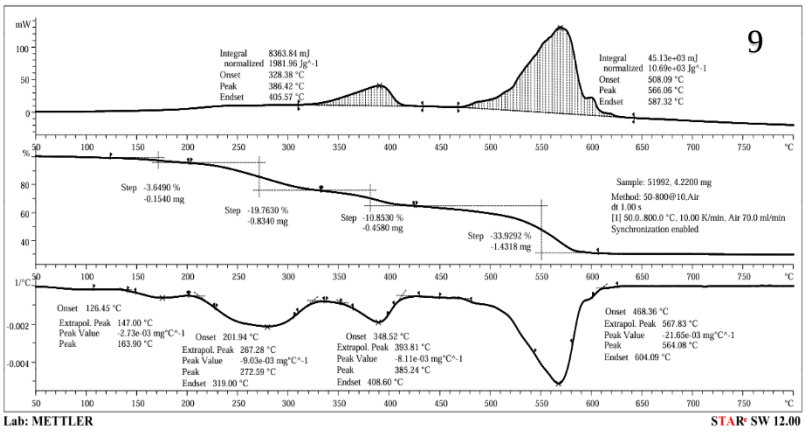

TGA spectra of complexes 5-9

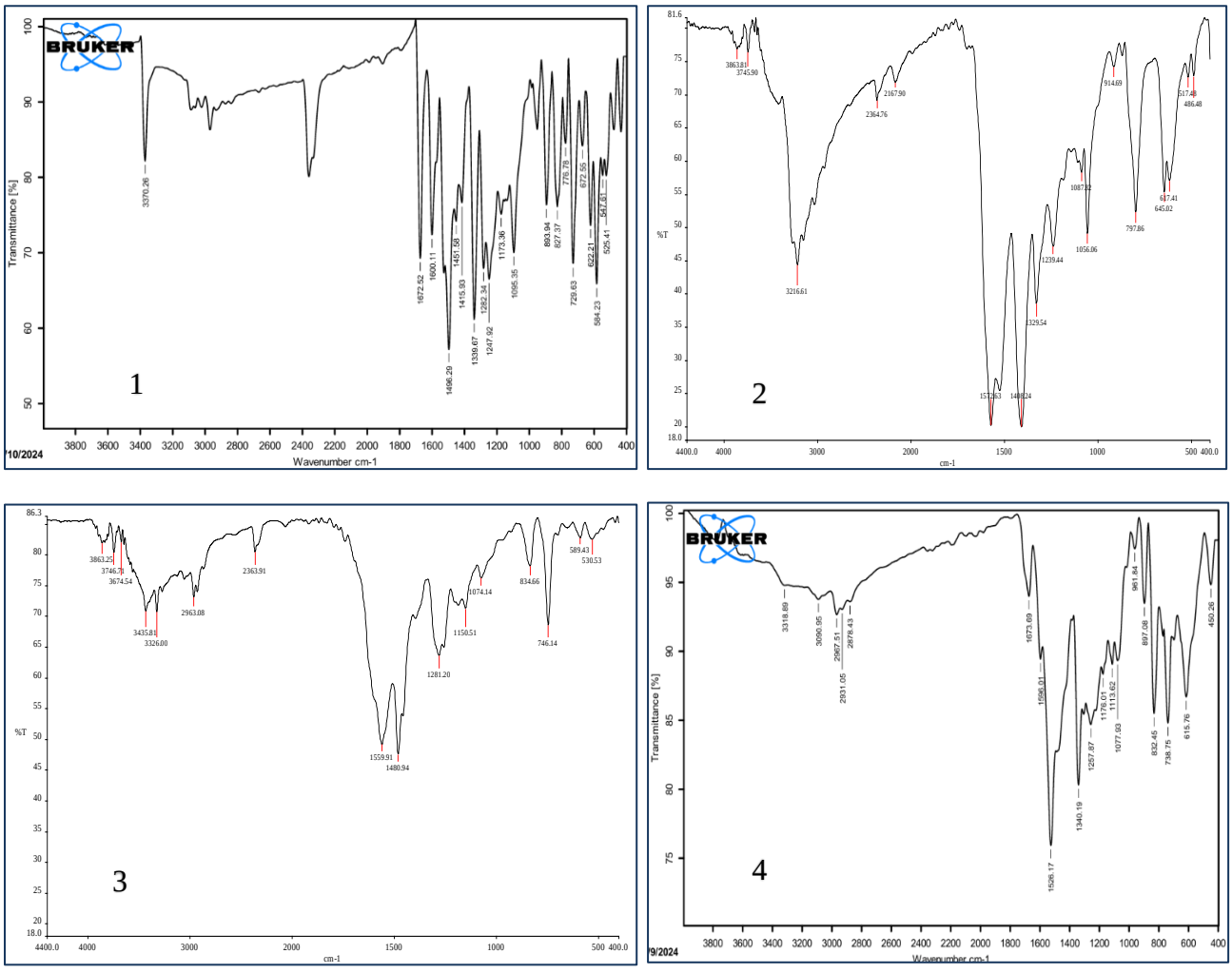

IR spectra of complexes 1-4

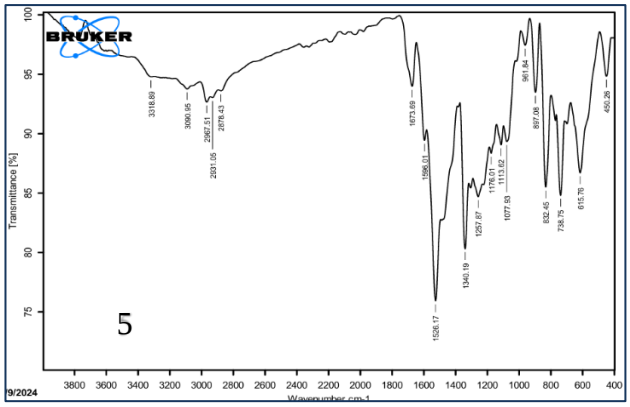

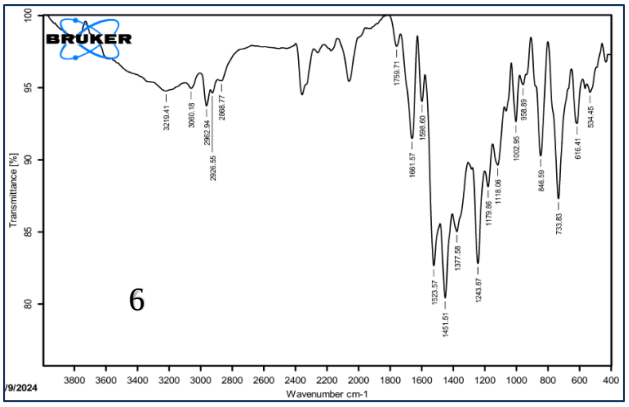

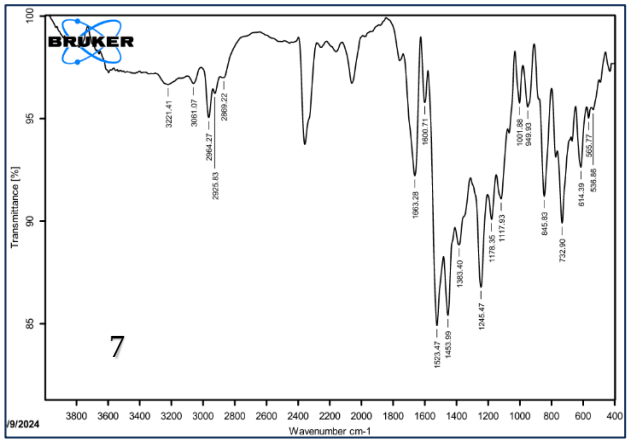

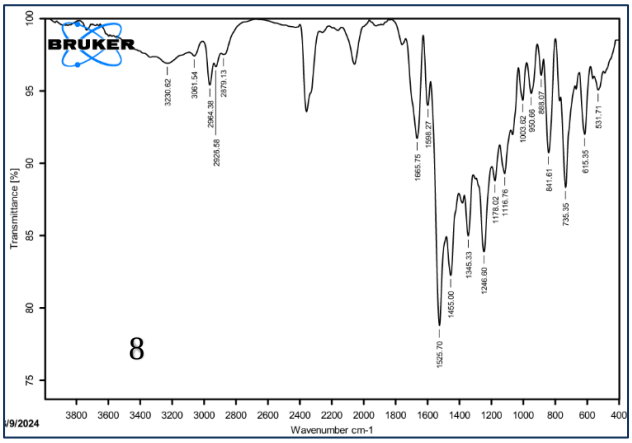

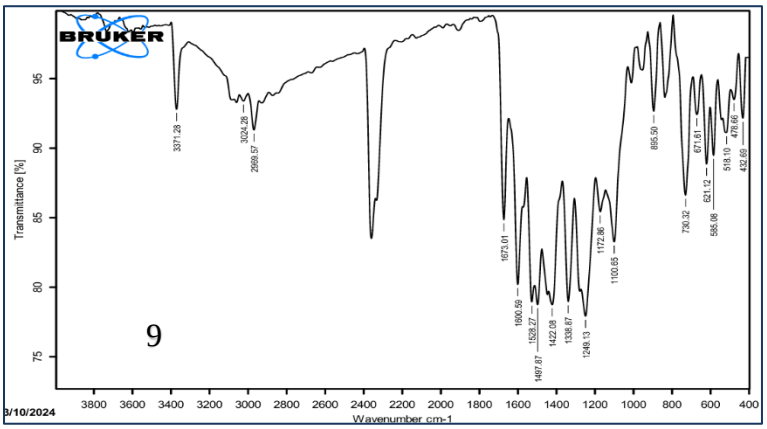

IR spectra of complexes 5-9

Journal of Basrah Researches (Sciences) **51**(2), 34 (2025)
DOI: https://doi.org/10.56714/bjrs.51.2.3

تحضير وتقييم النشاط المضاد لسرطان الثدي ودراسة الالتحام الجزيئي لمعقدات الكوبلت(II) والروثينيوم(III) المشتقة من مركبات البنزوايل ثايويوريا.

فاطمة غانم العلي، رافد حميدان الأسدي

قسم الكيمياء، كلية التربية للعلوم الصرفة، جامعة البصرة

معلومات البحث

الاستلام 6 تموز 2025
المراجعة 11 اب 2025
القبول 20 اب 2025
النشر 31 كانون أول 2025

الكلمات المفتاحية

بنزويل ثايويوريا ، خط خلايا سرطان الثدي(MCF-7) ، الالتحام الجزيئي، معقدات الكوبلت، معقدات الروثينيوم.

الملخص

تم تحضير سلسلة من معقدات الكوبلت والروثينيوم (1-9) المحتوية على مشتقات بنزويل ثايويوريا عن طريق تفاعل مشتقات 4-إيثيل بنزويل ثيويوريا مع أملاح الكوبلت والروثينيوم المائية بوجود القاعدة كربونات البوتاسيوم(K_2CO_3). عملت جزيئات الثيويوريا كليكندات ثنائية السن، حيث تم التناسق مع أيونات الفلزات من خلال ذرتي الكبريت والأوكسجين لكل من معقدات الكوبلت والروثينيوم. تم بنجاح تحضير هذه المعقدات وتشخيصها باستخدام عدة تقنيات تحليلية منها: مطيافية الأشعة تحت الحمراء(FT-IR)، التحليل الحراري الوزني(TGA)، قياسات الحساسية المغناطيسية، التوصيلية المولارية، والمطيافية الأشعة المرئية وفوق البنفسجية (UV-Vis) كما تم تقييم الفعالية البيولوجية للمعقدات من حيث قدرتها على تثبيط نمو الخلايا السرطانية ضد خط خلايا سرطان الثدي(MCF-7)، وقد أظهر المعقد 3 أعلى نسبة تثبيط. علاوة على ذلك، أظهرت دراسات الالتحام الجزيئي (Molecular Docking) لهذا المعقد امتلاكه لأعلى ألفة ارتباط مع بروتينات KCV5 وERT3، حيث سجل أقل طاقة ارتباط (Binding Energy) وأدنى قيم انحراف جذر تربيعي متوسط (RMSD)، مما يشير إلى ارتباط قوي ومستقر.

Citation: F. G. Al-Ali, R. H. Al-Asadi, J. Basrah Res. (Sci.) **50**(2), 34 (2025). DOI:https://doi.org/10.56714/bjrs.51.2.3

***Corresponding author email:** dr.rafid74@yahoo.com

ISSN: 1817-2695 (Print); 2411-524X (Online)
Online at: https://jou.jobrs.edu.iq